PROCESS MONITORING IN LASER SINTERING USING THERMAL IMAGING

A. Wegner* and G. Witt*
*Chair for Manufacturing Technology, Institute for Product Engineering, University of Duisburg Essen, Germany

REVIEWED, August 17 2011

Abstract

In laser sintering, inhomogeneous shrinkage, warpage, in-build curling and poor repeatability of part properties are well-known problems. All these effects are significantly influenced by the inhomogeneous temperature distribution on the powder bed surface. For this reason, it is often asked for the integration of additional measuring equipment into the machines for advanced process monitoring. In the research done, a thermal imaging system was successfully integrated into a laser sintering machine. Analyses were performed to understand the correlations between process parameters, the distribution of surface temperatures as well as the temperature of the melted material, and their influence on part properties.

Introduction

The laser sintering of plastic parts is, besides beam melting of metal parts, one of only two Additive Manufacturing processes which have the capability to be used in Rapid Manufacturing in the near future [1]. The powder bed surface in laser sintering is preheated to a temperature close to the material's melting point by a radiant heater [2]. The distribution of temperatures on the powder bed surface should be as homogeneous as possible to achieve equal part properties throughout the whole build space, minor part warpage and narrow tolerances. However, experience shows very inhomogeneous temperature distributions [3, 4]. Therefore, it is often asked for the integration of new process monitoring systems into the machines. Within a bilateral industrial project and a project funded by the German Research Foundation "DFG", thermal imaging has been chosen as a process monitoring system and has been integrated into a laser sintering machine. Thermal imaging allows a two-dimensional measurement of surface temperatures and can give information on the temperature of the powder bed surface. Additionally, thermal imaging allows for the monitoring of the temperatures, while the laser is working, and therefore it gives the possibility to establish correlations between process parameters and the melt's temperature.

State of the Art

Thermal imaging is no new measuring system in laser sintering. It has been used several times for the determination of temperatures and results have been published in different papers and theses. However, sometimes restrictions, regarding the informative value of the measurements, resulted from the chosen experimental setup. A very critical factor in thermal imaging is the angle between the camera's axis and the surface normal. There will be a rising deviation between the measured temperature value and the real temperature for increasing angles. This effect can be neglected up to angles of 30°, based on the information given by the manufacturer of thermal imaging cameras [5].

[6] measured the melt's temperature just after exposure to laser light as a function of different parameter sets and densities of energy. The results showed a linear correlation between the melt's temperature and density of energy. The measurement was done at room temperature without preheating and without an inert atmosphere. Thus, some important influences on the process may have been neglected in these measurements, resulting in possible deviations from the real laser sintering process. [7] analyzed surface temperatures and the melt's temperature when processing polystyrene. He measured the temperatures through the machine's viewing window using an observation angle of 60°. The viewing window is a laser protection window with a transmission of only 25 % in the wavelength range of the used thermal imaging system. Due to that test setup, the measured values will deviate from the real temperature on the powder bed surface. This test setup was improved in [3]. The original viewing window of a DTM Sinterstation 2500 was replaced by an assembly containing a zinc-selenide window, which has a high transmission in the wavelength range of the used thermal imaging system. The large viewing angle was kept in this solution. The analysis showed maximum temperature differences of 13 K on the part bed surface and 30 K on the outer ring of the radiant heater. A further application of thermal imaging is the measurement of the temperature deviation within the laser focus. [8] analyzed the laser focus while processing titanium and [9] did the same for polyvinyl alcohol.

The system manufacturers also develop some approaches for using thermal imaging for process monitoring and control. In a 3D-Systems-patented solution, a thermal imaging system replaces the typical IR-sensor for temperature control in laser sintering [10]. Arcam want to utilize the measured surface temperatures to control the beam power as a function of the measured temperature value [11]. [12] describes an approach in laser sintering using an IR-radiation picture for checking the powder surface's quality and the melted areas regarding completeness and position. At the catholic university of Leuven, a feedback control system was developed which is going to be integrated in Concept Laser's beam melting systems [13, 14]. The setup uses a high-speed CMOS-camera, a photodiode, the machine's scanner head and a semi-reflective mirror to measure the emitted radiation of the melt pool. While the laser is operating, the grey values are measured with the CMOS-camera and are correlated with the melt pool's temperature. Furthermore, the size of the melt pool is controlled by the photodiode. Both values allow for a permanent, stable and robust monitoring and feedback control of the laser beam melting process by an active adjustment of the laser's power [13, 14, 15]. Another solution of a temperature monitoring system for laser sintering and beam melting is presented in [16]. It uses a two-wavelength pyrometer for determining the temperature and a high-speed CCD-camera to measure the temperature distribution in the laser focus. For both processes, the temperature of the melt can be measured with sufficient optical resolution.

Experimental Setup

Two solutions following different aims are being developed to integrate a thermal imaging system into a laser sintering system DTM Sinterstation 2500. Both are based on conclusions from the literature research. A thermal imaging system InfraTec Jade III MWIR with an optical resolution of 320 x 240 pixels, a maximum temporal resolution of 700 Hz and a wavelength range from 3 – 5 µm is used for the analysis.

The first experimental setup allows for the observation of the entire powder bed surface (380 x 330 mm) for measuring the temperature distribution (cf.

Figure **1**). The x-y-scanner head is replaced by the thermal imaging system to observe the surface through the laser window. The angle between the camera's axis and the surface normal is 5°. A wide-angle lens with a focal distance of 12 mm is chosen for the measurement, resulting in an optical resolution of 1.5 mm per pixel on the powder bed surface. This resolution is sufficient to analyze the temperature distribution.

The second setup is placed adjacent to the scanner head with an observation angle of 23°. This setup permits making different measurements: Firstly, the temperature distribution on 2/3 of the powder bed surface can be measured using the wide-angle lens. Secondly, the measurement of the melt's temperature is possible while the laser is working. For this purpose, a telephoto lens with a focal distance of 50 mm is used, resulting in an optical resolution of 0.35 mm, which is smaller than the laser focus diameter of 0.45 mm. The ideal optical resolution per pixel for that measurement would be a maximum of 0.15 m m, which means that three pixels lie on a single scan line. As a result at least one pixel lies exactly on the scan line at any given time, hence displaying the real temperature. In case of 0.35 mm, one pixel can sometimes lie on two scan lines simultaneously, showing an average temperature of both lines. But the chosen standard hatch distance of 0.15 mm helps to avoid that problem in most cases. Additionally, six single measurements are performed for each parameter set to acquire precise temperature values. For future analysis, this effect is avoided completely by a new thermal imaging system with an optical resolution of 0.15 mm, having also a higher temporal resolution of 5000 Hz. The setup is chosen in contrast to state-of-the-art setups with a fixed field of view on the part surface. Unlike the solutions where the field of view is moving with the laser focus, this configuration offers the possibility to also analyze the cool-down of the melted area and the thermal distribution of a complete part. To avoid potential damage of the thermal imaging system by the CO_2-laser, a sapphire window is used which cuts off all radiation above 6 µm but has a very high transmission in the camera's wavelength range. Non-refreshed EOS PA 2200 powder is chosen for all analysis as reference material.

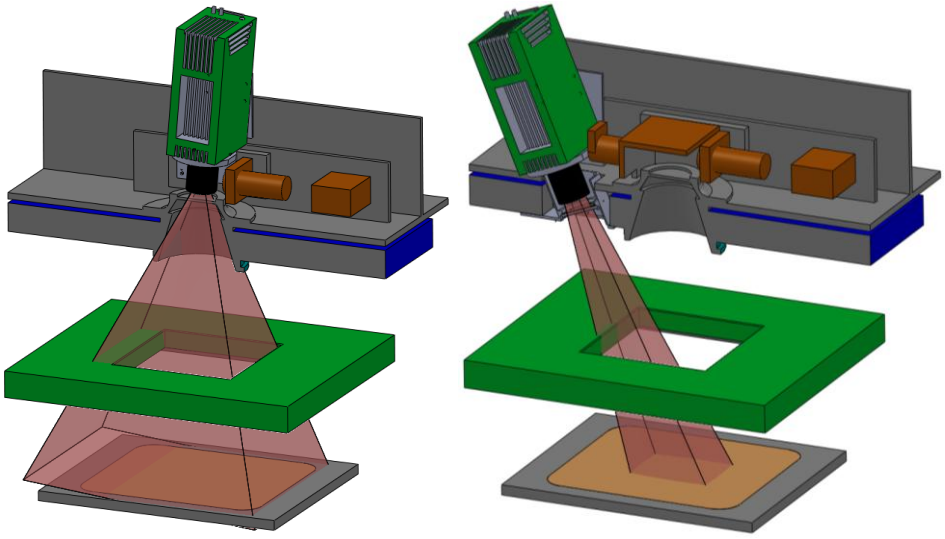

Figure 1. Left: Experimental setup one for temperature distribution
Right: Experimental setup two for melt's temperature

Radiant Heaters

The radiant heater positioned above the powder bed in a laser sintering machine provides for the preheating of the surface close to the material's melting point, setting up a temperature distribution as homogeneously as possible. Thereby, the temperature of the heater reaches temperatures significantly higher than the temperature of the powder bed surface. The produced heat energy is transferred to the powder bed by infrared radiation, where most of the radiation is absorbed. However, a part of the radiation is reflected by the surface. The temperature of the powder bed causes an infrared radiation itself, according to Planck's law [5]. Based on the chosen experimental setup, the emitted radiation of the powder bed as well as the reflected radiation of the heater are both measured by the thermal imaging system. Therefore, the temperature of the radiant heater has an influence on the measured temperature of the powder bed surface depending on its percentage of all radiation.

The radiant heater's temperatures of two different DTM Sinterstations 2500 have been measured depending on the power setting to quantify their influence. Additionally, the temperature distribution on the heaters' surfaces is analyzed to check their function. Figure 2 compares the average temperatures of different heater areas for a power setting of 30 %. The surfaces of the inner heater circuit show significantly lower temperatures in comparison to the outer heater circuit which are approximately 30 K hotter. The temperature differences within one heater circuit are significantly higher for the blue marked DTM 2500 compared to the machine marked with red. Thus, differences between the hottest and coldest heater area of the blue DTM 2500 are about 15 K for the outer circuit and even 20 K for the inner one. The values for the red machine are slightly lower being 13 K for the outer heater circuit and 10 K for the inner one.

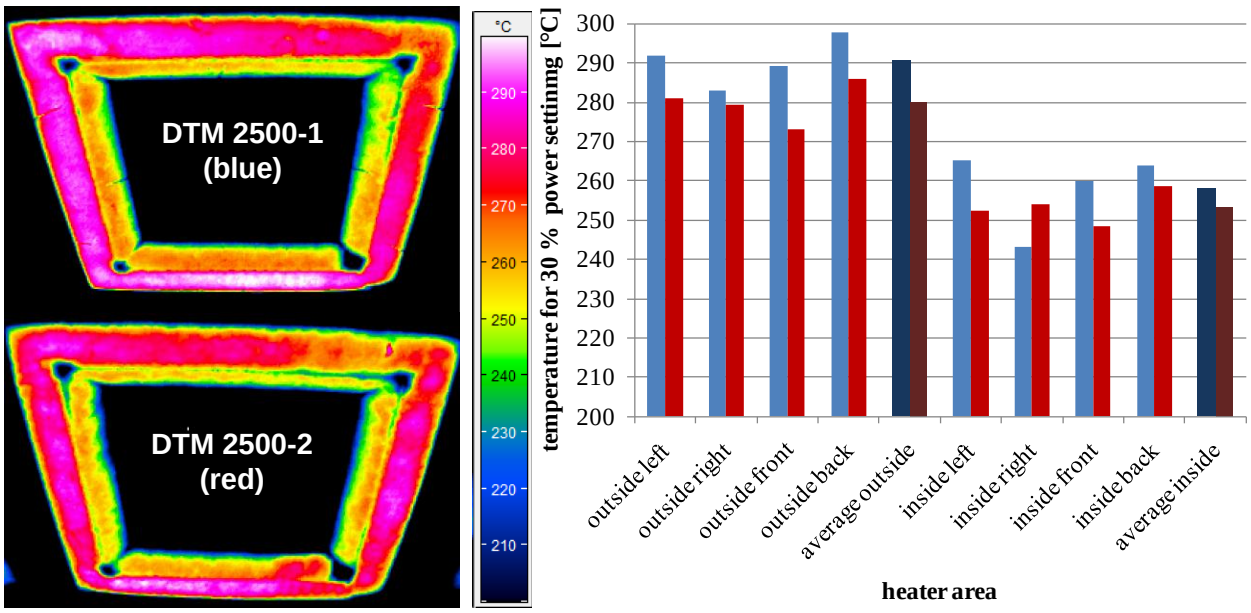

Figure 2. Comparison of different radiant heaters for 30 % power setting
Left: Thermal images of both heaters
Right: Comparison of the measured radiant heater temperature

The results also show that both radiant heaters have a very inhomogeneous temperature distribution. Therefore, these two heaters are not able to realize a homogenous temperature distribution on the powder bed surface. The results show that thermal imaging is a suitable measuring system to check the function and homogeneity of the radiant heaters in laser sintering.

In a second step, the stability of heater temperatures within the process is analyzed as a function of the cycle time. Figure 3 shows the time-dependant average heater temperature of the outer heater circuit for three different cycle times. The graph shows a significant difference between the heater's temperature levels for the three measured cycles. Additionally, the temperature deviation within a cycle increases significantly for longer cycle times. For cycle times of ten seconds, the deviation of the heater temperature is only about 4 K between two successive coating processes. This value increases to 14 K for a cycle time of sixty seconds. The results show that the heater temperature is not a stable value. This is caused by an increase of heater power setting when new, cold powder is deposited. After reaching the preheating temperature, the power is reduced in little steps to maintain this temperature level. This leads to decreasing heater temperatures until new powder is deposited. When making a thermal imaging measurement the ambient temperature has significant influence on the measured powder bed temperature. Due to that, it is necessary to log the heater temperature at all times.

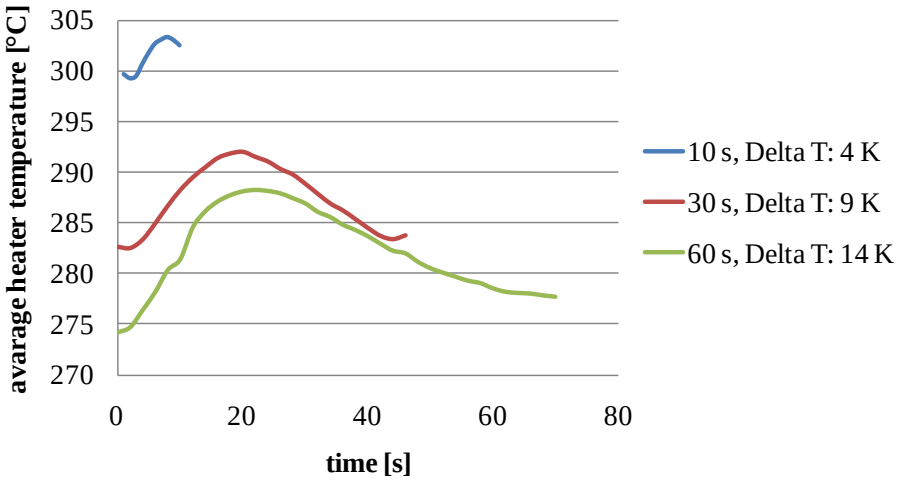

Figure 3. Time dependent average heater temperature for different cycle times

Temperature Distribution on the Powder Bed Surface

Based on the results for the radiant heaters, the temperature distribution on the powder bed surface is measured while the machine, flooded with nitrogen, is preheated. For this measurement, experimental setup one is used. The resulting temperature distribution is shown in Figure 4. The diagram illustrates a deviation between the minimum and maximum temperatures of 7.5 K. The reference temperature during the measurement is chosen as 174 °C, being close to the onset temperature determined by differential scanning calorimeter measurements for PA 2200 [17]. The machine's set-point temperature is 177 °C, which is determined via melting tests. However, this value is not feasible as a reference temperature because the machine's pyrometer generally does not show the real surface temperature due to an inaccurate calibration.

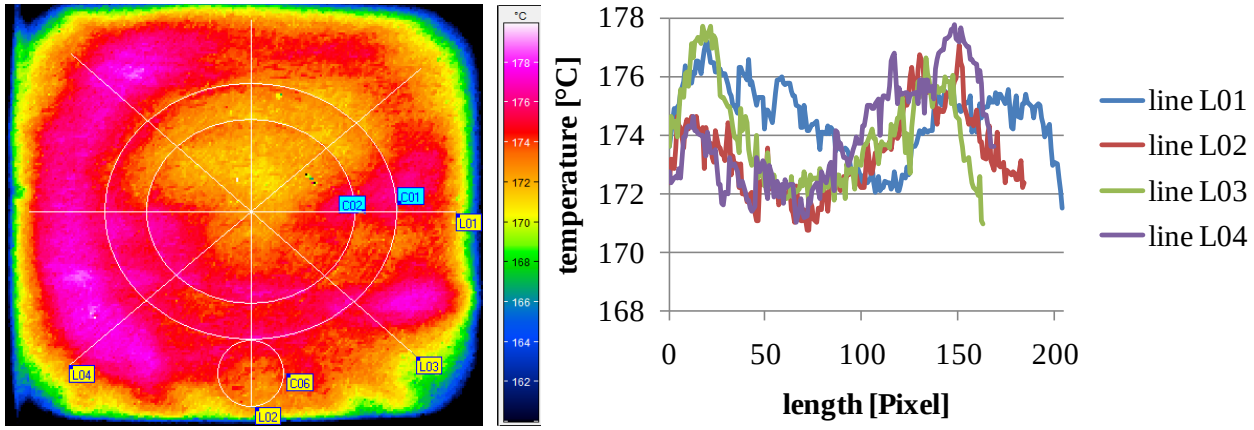

Figure 4. Temperature on the powder bed surface for a set-point temperature of 177 °C
Left: Thermal image of the temperature distribution
Right: Temperature deviation

In a second step, temperature distribution is analyzed as function of the build height. The temperature deviation is measured during the normal warm-up stage of 25 mm and the first 12 mm of a build job. At a height of 10 mm, the set-point temperature of 177 °C is reached for the first time. The graph in Figure 5 shows that correlation. The maximum deviation decreases significantly by 6.2 K within the warm-up stage and subsequently by 1.4 K within the first 12 mm of a build job, resulting in a temperature difference of 6.3 K for a build height of 12 mm. The average temperature deviation shows only a decrease by 4.4 K within the warm-up stage and then a decrease by another 1.6 K. The results prove that the standard 25 mm warm-up stage lasting about 2.5 hours is necessary to reduce the temperature deviation to an acceptable value for the laser sintering process.

Figure 5. Temperature deviation dependent on the build height

Measurement of the melt's temperature

Only little information is available about the melt's temperature in laser sintering. The analyses published give no detailed and precise information about the process and the

correlations between temperature and process parameters. This is due to the limitations of the experimental setup, or because the setup is only described theoretically with just few measured values. The analysis given in this paper shows first results describing the correlation between the melt's temperature and the process parameters.

In a first step, the fill laser power is increased stepwise to analyze its influence on the melt's temperature, while the other parameters kept at the standard values. The resulting graph (cf. Figure 6) shows a linear correlation, which proves the analysis done by Keller [7]. A raise of laser power by 1 W results in an increase of temperature by approximately 4.44 K. When the graph is extrapolated to lower laser power values, the melting point of PA 2200 at 184,3 °C [17] is reached when using a laser power of about 6.5 W, which correlates to a density of energy of 0.85 J/cm². The literature indicates slightly higher densities of energy, namely at least 1.0 J/cm², at which sintering occurs [18]. When adding a second exposure to the laser light, the melt's temperature increases by 30 K. The first exposure of a double exposure results in the same temperature values as a single exposure. All thermal images show a sharp border between the melted area and the surrounding unmelted powder. Due to this fact, thermal imaging with a fixed field of view is suitable for checking the melted areas on the powder bed surface in comparison to the layer data in general.

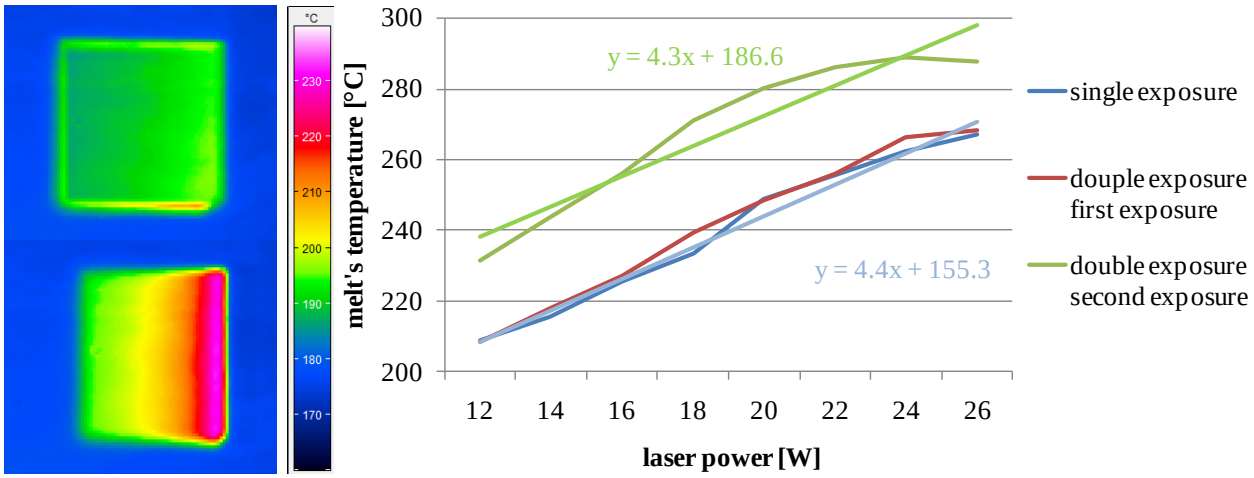

Figure 6. Left: Outline scan with 3.5 W and fill scan with 16 W
Right: Average temperatures of the melt for single scan lines depending on the laser power

In a second step, the influence of part size on the melt's temperature is analyzed. It is well known that mechanical properties of tensile bars depend on the part's orientation in the xy-plane when not using the cross fill scan strategy, due to the different scan vector lengths [4, 19]. Figure 7 gives the correlation of the melt's temperature and the part size for two different laser power values. The graph shows a maximum temperature for parts with a length of 5 mm. The temperature decreases with increasing part lengths. This in turn correlates to an increasing scan vector length and a longer scan time. The value for 20 mm part length is identical to the results shown in Figure 6. The graph also gives the temperature values for the width (10 mm) and the length (150 mm) of a standard tensile bar (DIN EN ISO 527-2). These values correlate with the production of tensile bars when scanning only in either x-direction or y-direction without using

the cross fill scan strategy. There is a significant temperature difference of 20 K and 36 K for a laser power of 14 W, respectively 18 W when comparing the melts' temperatures for the two different scan directions. This correlates to a laser power difference of 4.5 W in the first case and of even 8 W in the second case. These results show, for the first time, a reason for the well-known dependency of mechanical properties on part orientation by comparing the maximum temperature of the melt while scanning parts with different scan vector lengths.

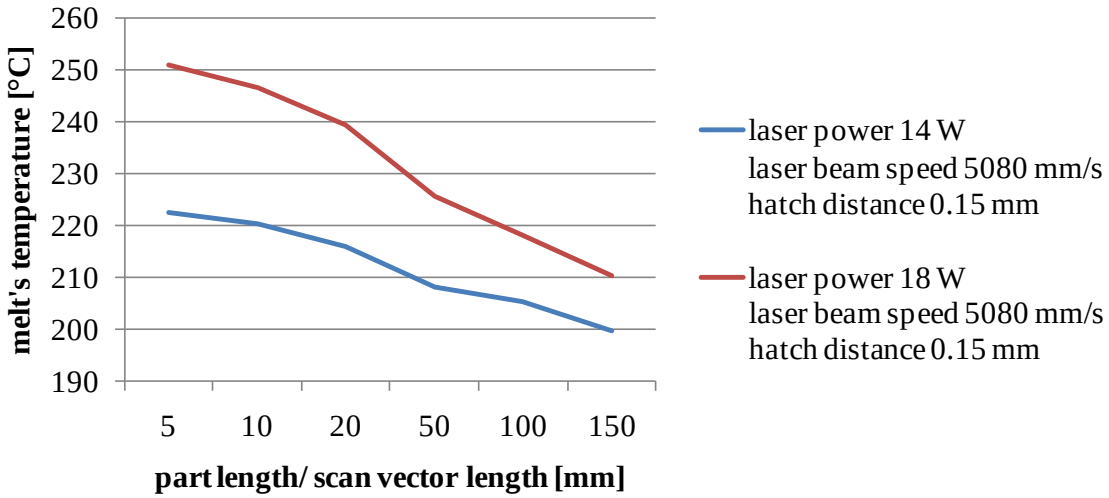

Figure 7. Melt's temperature plotted against scan vector length

The equation for the density of energy is well-known for the description of the correlation between energy input E, laser power P, laser beam speed v and the hatch distance h [6, 18]:

$$E = \frac{P}{v \cdot h}$$

Different publications give information indicating that this correlation does not always apply. Parts which are built with the same density of energy but using different parameter sets also show different mechanical properties [19]. Due to those results, the correlation between the density of energy, different parameter sets and the melt's temperature are analyzed using thermal imaging. The results are shown in Figure 8. The graph shows an almost linear correlation between the laser beam speed and the melt's temperature with a slope of 2.5 K per 1000 mm/s. For the hatch distance, there is only a slight increase in temperature of 4 K for 2.0 W/cm² while for 2.5 W/cm² the temperature even decreases for a hatch distance of 0.25. This may be caused by the quality and age of the used laser and should be analyzed in future analyses. Thus, there is no obvious tendency for a correlation between the hatch distance and the melt's temperature. Comparing both diagrams, the maximum temperature deviation is about 11 K, while the density of energy is kept constant. This relatively high deviation of the melt's temperature is a possible reason for the deviations of the mechanical properties described in the literature. Therefore, the equation describes the correlations in laser sintering insufficiently.

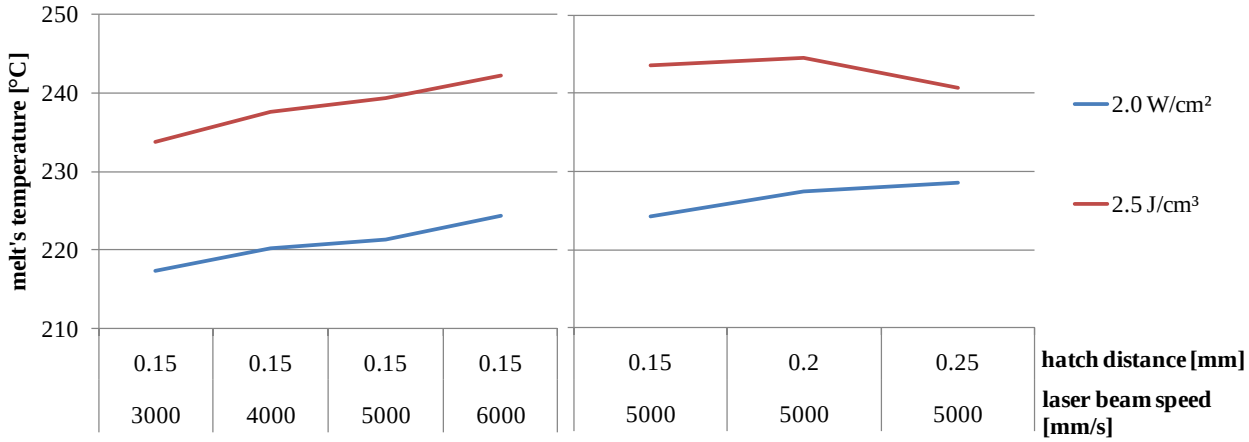

Figure 8. Melt's temperature plotted against the laser beam speed respectively the hatch distance for constant density of energy

Conclusion and Outlook

Within the scope of the analysis carried out, a thermal imaging system was successfully integrated in a laser sintering machine. At the same time, necessary solutions were developed for the problems which emerged from the integration of the system, like the measurement of the radiant heater's temperature. Afterwards, the temperature distribution on the part bed surface was determined. Additionally, influence factors on the homogeneity of the surface's temperature were analysed. Further analysis was done to determine the melt's temperature as a function of different process parameters. The results show that thermal imaging has different possible application in laser sintering. Thermal imaging is suited for process monitoring of the powder bed surface temperature distribution and the melt's temperature. Another application is the checking of the radiant heater's function and homogeneity during a regular service. Thereby, cold areas on the surface can be detected and can be considered in pre-processing.

In the future, the temperature distribution of different available laser sintering systems should be compared, using the results mentioned, to develop an optimized heater system. Additionally, fundamental correlations between process parameters, the melt's temperature and the part properties should be analyzed using the new thermal imaging system with better optical and temporal resolution.

Acknowledgment

The authors would like to thank the German Research Foundation DFG for funding the research within the research project "Fundamentals for a Quality Assurance System applied to Rapid Manufacturing Processes".

Literature

[1] N., N.: Additive fabrication – Rapid technologies (rapid prototyping) – Fundamentals, terms and definitions, quality parameters, supply agreements, VDI-Guideline 3404, Association of German Engineers, 2009.

[2] Gebhardt, A.: Generative Fertigungsverfahren – Rapid Prototyping – Rapid Tooling – Rapid Manufacturing, 3. Edition, Munich, Hanser Publishing, 2007.
[3] Diller, T.; Sreenivasan, R.; Beaman, J.; Bourell, D.; LaRocco, J.: Thermal model of the build environment for polyamide powder selective laser sintering, In: Bourell, D. (Editor): Proceedings of the 21st Annual International Solid Freeform Fabrication Symposium (SSF 2010): The University of Texas at Austin 2010, pp. 539-548.
[4] Sauer, A.: Optimierung der Bauteileigenschaften beim Selektiven Lasersintern von Thermoplasten, PhD thesis; University of Duisburg-Essen, 2005.
[5] N., N.: Einführung in Theorie und Praxis der Infrarot-Thermographie, InfraTec, 2011.
[6] Keller, B.: Rapid Prototyping: Grundlagen zum selektiven Lasersintern von Polymerpulver, PhD thesis, university of Stuttgart, 1998.
[7] Nöken, S.: Technologie des Selektiven Lasersinterns von Thermoplasten, PhD thesis, RWTH Aachen, 1997.
[8] Kosolov, S.; Boillat, E.; Glardon, R.; Fischer, P.; Locher, M.: 3D FE simulation for temperature evolution in the selective laser sintering process, In: International Journal of Machine Tools & Manufacture, 44 (2004), pp. 117-123.
[9] Wiria, F. E.; Leong, K. F.; Chua, C. K.: Modeling of powder particle heat transfer process in selective laser sintering for fabricating tissue engineering scaffolds, In: Rapid Prototyping Journal, 16 (2010) 6, pp. 400-410.
[10] Chung, M.; Allanic, A.-L.: Sintern unter Verwendung von Thermobild-Rückkopplung. patent DE102004017769B4, 3D Systems Inc., 2004.
[11] Andersson, L.-E.; Larsson, M.: Vorrichtung und Anordnung zur Herstellung eines dreidimensionalen Objekts, patent DE60108390T2, Arcam AB, 2001.
[12] Philippi, J.: Verfahren zum Herstellen eines dreidimensionalen Objekts mittels Lasersintern, patent DE102007056984A1, EOS GmbH, 2007.
[13] Kruth, J.P.; Mercelis, P.; Van Vaerenbergh, J.; Craeghs, T.: Feedback control of selective laser melting; In: Bartolo, P. J. et al. (Editor): Virtual and Rapid Manufacturing - Advanced Research in Virtual and Rapid Prototyping: Taylor and Francis 2007, pp. 521-527.
[14] Craeghs, T.; Bechmann, F.; Berumen, S.; Kruth, J.-P.: Feedback control of Layerwise Laser Melting using optical sensors, In: Physics Procedia, 5 (2010), pp. 505-514.
[15] Berumen, S.; Bechmann, F.; Lindner, D.; Kruth, J.-P.; Craeghs, T.: Quality control of laser- and powder bed-based Additive Manufacturing (AM) technologies, In: Physics Procedia, 5 (2010), pp. 617-622.
[16] Chivel, Y.; Smurov, I.: On-line temperature monitoring in selctive laser sintering/ melting, In: Physics Procedia, 5 (2010), pp. 515-521.
[17] Drummer, D.; Rietzel, D.; Kühnlein, F.: Development of a characterization approach for the sintering behavior of new thermoplastics for selective laser sintering, In: Physics Procedia, 5 (2010), pp. 533-542.
[18] Bacchewar, P. B.; Singhal, S. K.; Pandey, P. M.: Statistical modeling and optimization of surface roughness in the selective laser sintering process, Proceedings of the Institution of Mechanical Engineers, Part B: Journal of Engineering Manufacture, 221 (2007) 1, pp. 35-52.
[19] Kaddar, W.: Die generative Fertigung mittels Laser-Sintern: Scanstrategien, Einflüsse verschiedener Prozessparameter auf die mechanischen und optischen Eigenschaften beim LS von Thermoplasten und deren Nachbearbeitungsmöglichkeiten, PhD thesis, University of Duisburg-Essen, 2010.